CHEMICAL ENGINEERING TRANSACTIONS
VOL. 99, 2023
A publication of AIDIC
The Italian Association of Chemical Engineering
Online at www.cetjournal.it
Guest Editors: Sauro Pierucci, Flavio Manenti

ISBN 978-88-95608-98-3; **ISSN** 2283-9216
DOI: 10.3303/CET2399070

Analysis of High Temperature Degradation of Multi-Layer Insulation (MLI) Systems for Liquid Hydrogen Storage Tanks

Davide Camplese[a,*], Carmela Chianese[a], Giordano Emrys Scarponi[a], Robert Eberwein[b], Frank Otremba[b], Valerio Cozzani[a]

[a]Alma Mater Studiorum - Università di Bologna, Dipartimento di Ingegneria Civile, Chimica, Ambientale e dei Materiali, via Terracini 28, 40131 Bologna, Italy
[b]Bundesanstalt für Materialforschung und -prüfung (BAM), Berlin
davide.camplese@unibo.it

The interest in hydrogen-based green energy is increasing worldwide, and the same is true for hydrogen-powered vehicles. Among the possible solutions to store hydrogen in such vehicles, cryogenic tanks equipped with multi-layer insulation (MLI) are the most promising to increase the amount of energy stored per unit volume. However, MLI is affected by severe deterioration when exposed to an external source of heat such as a fire following a car accident, leaving the tank unprotected and leading to failure in a relatively short time. In this work, a one-dimensional model to evaluate MLI thermal degradation when a liquid hydrogen tank is exposed to fire is presented. The relevance of taking MLI degradation into account when simulating the pressure increase due to external fire exposure is here demonstrated through the analysis of several case studies. The results show that MLI systems performance depletes within a few minutes of exposure to hydrocarbon poolfire.

1. Introduction

Hydrogen is among the most promising candidates to replace fossil fuels in the energy transition (Preuster et al., 2017). Hydrogen-powered vehicles are already a reality and their number is foreseen to increase considerably in the next decade.

Among the possible solutions to store hydrogen in vehicles, cryogenic storage tanks appear to be the most effective to ensure high volumetric energy density (Kunze & Kircher, 2012). Since cryogenic storage conditions as well as low boil-off rates have to be maintained for a prolonged time, the heat leakage towards the tank must be kept at minimum values. For this purpose, several types of thermal superinsulation systems such as perlite, high-vacuum, and multi-layer insulation (MLI) were developed. In particular, MLI systems are one of the most suitable as they can strongly reduce heat leakage into the vessel with a thinner thickness if compared to other insulation materials (Edward & Filip, 2018). The advantages of cryogenic storage come together with potential risks due to hydrogen's high flammability.

An accidental loss of integrity of liquefied hydrogen storage units might lead to extremely dangerous phenomena, such as BLEVEs (Boiling Liquid Expanding Vapor Explosion) and fireballs (van Wingerden et al., 2022). In the transportation sector, one of the most critical scenarios that can threaten tank integrity is represented by the exposure to an external source of heat such as a fire developed as a consequence of a car accident. Despite the super insulation features of MLI, real-scale fire test results showed that cryogenic tanks featuring this type of system fail in a relatively short time (Pehr K., 1996). As demonstrated in the tests conducted by Eberwein et al. (2023), this is due to the strong degradation of MLI at high temperatures. This phenomenon causes the deterioration of MLI protective performance, leaving the tank almost unprotected against the high heat flux from the fire. As a consequence, the tank pressure undergoes a rapid increase which can finally lead to catastrophic failure. In this sense, the availability of accurate and robust models able to simulate such scenarios is a key element to ensure a safe design. Both CFD and zone models were proposed for this purpose (Scarponi et al., 2022), which provide satisfactory predictions when used to simulate pressure tank response to fire. However, none of them was designed to take into account the thermal degradation of the insulation system.

Paper Received: 10 January 2023; Revised: 17 March 2023; Accepted: 24 April 2023
Please cite this article as: Camplese D., Chianese C., Scarponi G.E., Eberwein R., Otremba F., Cozzani V., 2023, Analysis of High Temperature Degradation of Multi-layer Insulation (MLI) Systems for Liquid Hydrogen Storage Tanks, Chemical Engineering Transactions, 99, 415-420 DOI:10.3303/CET2399070

On the other hand, thermal models able to simulate the heat flux throughout the MLI (e.g., the one proposed by McIntosh, 1994) were developed and validated for normal operative conditions only, not accounting for insulation performance deterioration at high temperature.
The present work proposes a modelling approach for simulating the thermal degradation phenomena taking place at high temperatures in a typical MLI system. The aim is to provide a tool that can be integrated into CFD and zone models for the simulation of the response of cryogenic liquid tanks to fire exposure. The relevance of MLI degradation and its impact on the pressurization rate of a typical tank for hydrogen-powered vehicles under fire attack is demonstrated through the analysis of a series of case studies.

2. Methodology

MLI systems are composed of several layers of low-emissivity material (radiative layers) interleaved with high-free volume spacers. These are enclosed within the vessel double walled shell, working under high-vacuum conditions. The MLI thermal degradation model presented in this study subdivides the tank into *N*+3 nodes, as depicted in Figure 1. A node is assigned to each one of the *N* radiative layers. The internal and external shells are represented by node S_i and *Se*, respectively. Finally, node *L*, representative of the liquid hydrogen thermal behavior, is included to simulate the tank self-pressurization rate. A transient thermal heat balance equation is written for each node (eq. 1 to 6 in Table 1).

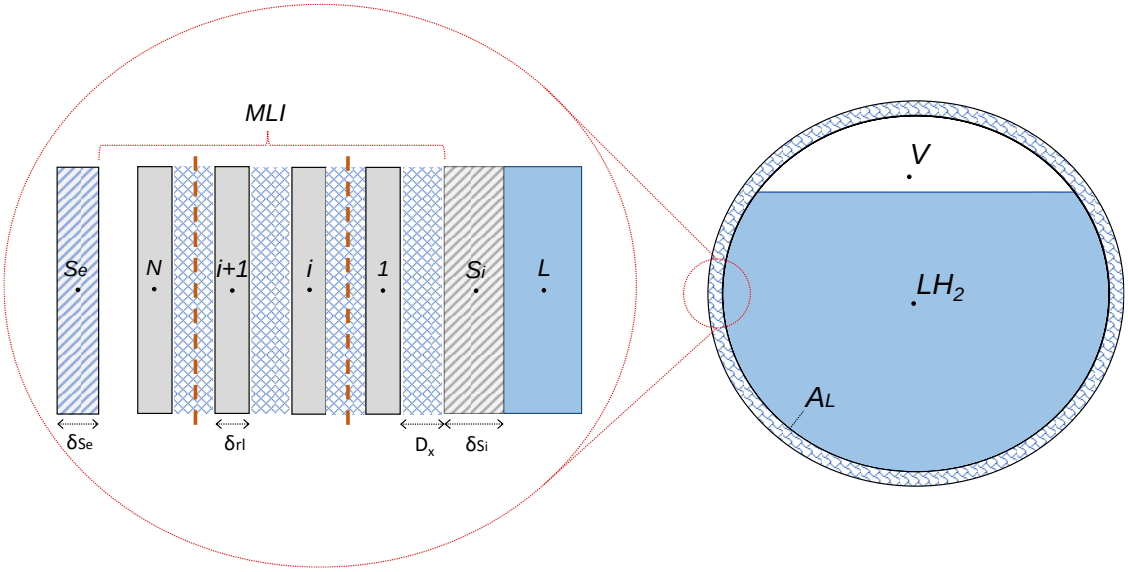

Figure 1. Schematic representation of the thermal node discretization. L = liquid, Se = external shell, Si = internal shell, rl = radiative layer. Nodes 1 to N refer to the MLI radiative layers.

Table 1. Set of the equation used for the MLI thermal degradation model.

Node	Variable	Equation	Eq. N°
S_e	T_{Se}	$\delta_{S_e}\rho_{S_e}c_{p\_S_e}\frac{dT_{S_e}}{dt} = \varepsilon_{S_e}\sigma\left(T_{BB\_fire}^4 - T_{S_e}^4\right) - \frac{1}{\left(\frac{1}{\varepsilon_{S_e}}+\frac{1}{\varepsilon_N}-1\right)}\sigma\left(T_{S_e}^4 - T_N^4\right)$	(1)
N	T_N	$\delta_{rl}\rho_{rl}c_{p\_rl}\frac{dT_N}{dt} = \frac{1}{\left(\frac{1}{\varepsilon_{S_e}}+\frac{1}{\varepsilon_N}-1\right)}\sigma\left(T_{S_e}^4 - T_N^4\right) - \mathrm{q}_{rl}^N$	(2)
i	T_i	$\delta_{rl}\rho_{rl}c_{p\_rl}\frac{dT_i}{dt} = \mathrm{q}_{rl}^{i+1} - \mathrm{q}_{rl}^i$	(3)
1	T_1	$\delta_{rl}\rho_{rl}c_{p\_rl}\frac{dT_1}{dt} = \mathrm{q}_{rl}^2 - \mathrm{q}_{rl}^1$	(4)
S_i	T_{Si}	$\delta_{S_i}\rho_{S_i}c_{p\_S_i}\frac{dT_{S_i}}{dt} = \mathrm{q}_{rl}^1 - h_L\left(T_{S_i} - T_L\right)$	(5)
L	T_L	$m_L c_{p\_L}\frac{dT_L}{dt} = A_L h_L\left(T_{S_i} - T_L\right)$	(6)
-	P	$P = P^*(T_L)$	(7)

The heat transfer is considered to occur only in the direction normal to the surface of the layer, resulting in a one-dimensional approach. The heat flux between any adjacent layer is expressed according to the classical "layer by layer" model proposed by McIntosh (1994), in which three mechanisms of heat transfer contribute to the total heat flux: the thermal radiation between each layer (q_{rad}, eq. 8), the solid conduction through the spacer material ($q_{s,cond}$, eq. 9), and the gas conduction through the spacer material ($q_{g,cond}$, eq. 10 and 11). Thus, the total heat flux from the i-th radiative layer to the (i-1)-th one is calculated according to eq. 12.

$$q_{rad}^{i} = \frac{\sigma}{\left(\frac{1}{\varepsilon_i} + \frac{1}{\varepsilon_{i-1}} - 1\right)}\left(T_i^4 - T_{i-1}^4\right) \tag{8}$$

$$q_{s,cond}^{i} = \frac{C_2 f k_s}{D_x}(T_i - T_{i-1}) \tag{9}$$

$$q_{g,cond}^{i} = C_1 P_r \theta (T_i - T_{i-1}) \tag{10}$$

$$C_1 = \left[\frac{\gamma + 1}{\gamma - 1}\right]\left[\frac{R}{8\pi M T}\right]^{1/2} \tag{11}$$

$$\mathrm{q}_{rl}^{i} = q_{rad}^{i} + q_{s,cond}^{i} + q_{g,cond}^{i} \tag{12}$$

The form of the thermal balance is the same for all the *N* nodes, except for the 1-st and the N-th ones. In fact, these face the inner and outer shells, respectively. Since the model assumes the 1-st radiative layer is separated from the inner shell by a single spacer, the thermal balance in node 1 preserves the same form as those shown for the other radiative layers, but eq. 5 has to be modified taking into account the emissivity of the inner shell surface material. On the contrary, a high-vacuum gap is present between the N-th and the S_e nodes, thus only radiative heat flux is considered to enter into the N-th radiative layer in eq. 2.

The novelty with respect to the classical layer by layer model is that the high temperature degradation of the MLI is taken into account by assuming that each radiation layer is destroyed when its temperature reaches the melting point of the material (here defined as the degradation temperature, T_{deg}). This assumption is dictated by logic that, when the i-th layer melts, it loses its shape, leaving the underlying layer unprotected. For simplicity, each layer is considered to be entirely and instantaneously destroyed as soon as exceeds T_{deg}. From the numerical model point of view, this phenomenon is simulated by replacing both the i-th radiative layer and the i-th spacer with a vacuum space of the same thickness. In this way, only radiative heat transfer is considered to take place between the first undamaged layer and the external shell. Such a procedure allows to take into account the gradual deterioration of the MLI system with the time.

The heat transfer from the fire is simulated by assuming that the external wall is uniformly exposed to thermal radiation from a constant black body temperature (T_{BB_fire}).

The tank pressure is assumed to match the saturation pressure (see Eq. 7 in Table 1) at the liquid temperature (T_L), calculated from the energy balance to the liquid node (see Eq. 6 in Table 1). The nucleate boiling heat transfer coefficient (h_L) is calculated according to eq. 13 (Ray, 1994), where P_c and $T_{L,sat}$ are the hydrogen critical pressure and liquid saturation temperature, respectively. Here it is assumed that the liquid is saturated (thus, $T_{L,sat} = T_L$).

$$h_L = \left(3.75 \times 10^{-5} P_c^{0.69}\left(T_{Si} - T_{L,sat}\right)^{0.7}\left(1.8\left(\frac{P}{P_c}\right)^{0.17} + 4\left(\frac{P}{P_c}\right)^{1.2} + 18\left(\frac{P}{P_c}\right)^{10}\right)\right)^{3.33} \tag{13}$$

The vapor phase is considered to be in thermodynamic equilibrium with the liquid one (i.e. liquid and vapor share the same temperature and pressure). Thus, no thermal balance is solved for this phase.

3. Case study

The thermal degradation model of MLI proposed in this study is applied to a horizontal cylindrical tank with two elliptical ends, an internal diameter of 0.6 m and a length of 1.2 m, for a total capacity of 0.31 m^3. These dimensions are representative of most storage tanks used for cryogenic hydrogen-powered vehicles. It is considered that 80 % of the storage volume is filled with liquid hydrogen at saturation temperature at ambient pressure (T_L = -252.75 °C, from NIST Chemistry WebBook). The thicknesses of the external and internal shells

are 0.003 m and 0.01 m, respectively. Their material properties are listed in Table 2 and are assumed to be constant throughout the simulation.

Table 2. Material properties.

Property	Symbol	Unit	Tank lading	External shell	Internal shell
Material/Compounds	-	-	Liquid hydrogen	AISI-304	AISI 316L
Density	ρ	kg/m^3	70.9*	7800	7900
Thermal Conductivity	k	W/(m·K)	-	16	15
Heat capacity	cp	J/(kg·K)	9800*	490	500
Emissivity	ε	-		0.9	0.275
* NIST, NIST Chemistry WebBook					

The tank features a typical commercial uniform density MLI composed of 20 pure aluminum radiative layers, interleaved with 20 layers of glass fiber fleece spacer material and a nominal area weight of 1.08 kg/m^2. Residual gas within the MLI is air. All the other data needed to close the model set of equations for the specific MLI considered are listed in Table 3.
The degradation temperature (T_{deg}) was set to 660 °C, which is the melting point temperature of the aluminum. A full engulfing hydrocarbon pool fire is selected as fire scenario. Thus, following the guidelines proposed by Anderson et al. (1974) and Birk et al. (2016), the T_{BB_fire} is set to 871 °C.

Table 3. MLI geometrical and material properties

Property	Symbol	Unit	Radiative layer	Spacer
Material	-	-	Aluminum	Glass fiber fleece
Thickness	δ_{rl}/D_x	m	$9\cdot10^{-6}$	$7\cdot10^{-4}$
Density	ρ	kg/m^3	2700	2500*
Thermal Conductivity	k	W/(m·K)	250	0.8*
Heat capacity	c_p	J/(kg·K)	900	-
Relative density	f	-	-	0.017
Emissivity	ε	-	0.04	-
Spacer empirical factor	C_2	-	-	0.0025
Residual gas pressure	P_r	Pa	$1\cdot10^{-4}$	
*solid material properties				

In order to assess the impact that the degradation of the MLI system can have on the pressurization rate of a cryogenic hydrogen tank in case of fire, three different cases were analyzed. In CASE A the degradation of MLI is simulated taking into account MLI degradation as described in section 2. Then, two limit conditions are considered. The first one (CASE B) assumes that MLI never degrades during exposure to fire, effectively keeping all radiative layers intact. In the second limit case (CASE C), no MLI is present, in fact considering only high vacuum between the two shells. Table 4 summarizes the simulations performed.

Table 4. List of case studies considered in the simulation.

Case study	Description
CASE A	MLI degradation on
CASE B	NO MLI degradation
CASE C	NO MLI presence in the vacuum chamber

In all the cases, the initial temperature profile in each node is set as the steady-state solution obtained considering constant boundary temperatures: a liquid temperature of -252.75 °C (i.e. the saturation temperature of hydrogen at atmospheric pressure) and an outer shell temperature of 25 °C (ambient temperature). This is representative of the system condition prior to fire exposure.

4. Results and Discussion

Figure 2 shows the transient temperature evolution within the tank insulation system obtained for CASE A. For the sake of clarity, only five radiative layers of the MLI are represented. The dashed red line depicts the temperature of the external wall. Starting from the initial value, this rapidly increases approaching the fire temperature. As a result, the temperature of the first MLI layer (solid yellow line) starts to rise until it reaches the

point of degradation (T_{deg}). At this point, when the layer is removed from the simulation, the underneath MLI layers are affected by the external shell temperature variation with a delay that is longer the further the layer is from the fire. It is worth noticing that, apart from the outermost layer, the rate of temperature increase of each radiative layer rises sharply as soon as the overlying layer is destroyed. In fact, when the i-th layer disappears, the (i-1)-th is suddenly exposed to high heat flux from the hot external wall. This phenomenon progresses until all the layers are destroyed. In the present simulation, this happens after 240 s of fire exposure. The dashed blue line depicts the temperature of the inner shell. Its value does not vary appreciably from the initial one as long as the entire MLI is not degraded. Since T_{Si} directly affects the heat flow entering the liquid phase (eq. 6 in Table 1), this means that the temperature of the tank lading does not change from its initial value until the entire MLI is destroyed. This demonstrates the protective effect of the MLI on tank lading in terms of delaying the temperature and, consequently, the pressure rise of the liquid hydrogen.

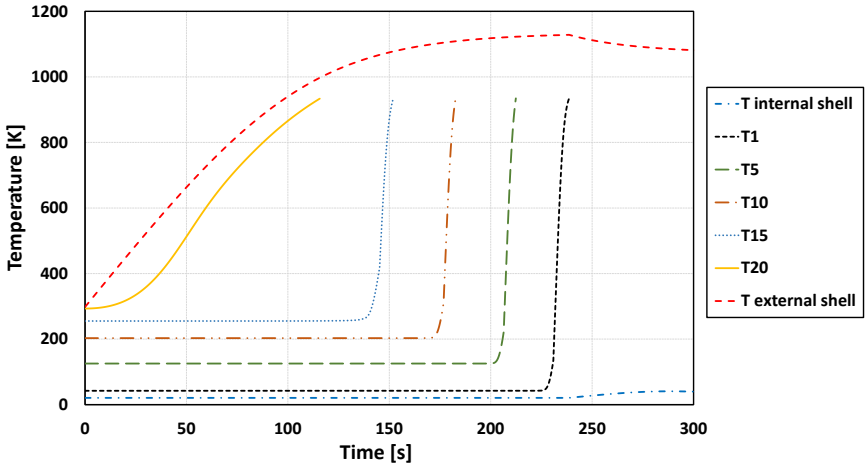

Figure 2. Transient temperature profile within MLI for simulation case A

Figure 3 shows the pressurization curves for the three case studies. When the MLI is not present (CASE C), the pressure inside the tank starts to grow up considerably earlier than in the cases in which the insulation system is in place. If the degradation of the MLI is not modelled (CASE B), the pressure increase over the simulation time is negligible. Clearly enough, this result is not realistic. On the other hand, if MLI degradation is taken into account (CASE A), the pressure increase comes with a significant delay if compared to CASE C. In other words, the MLI delays the time at which the “heat wave” from the fire reaches the liquid, resulting in a delayed pressure growth with respect to CASE C. These outcomes agree with what was observed by Eberwein et al. (2023).

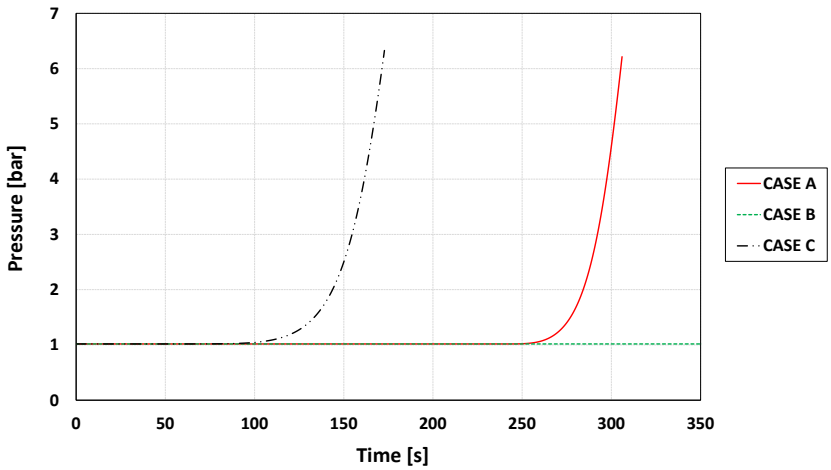

Figure 3. Pressurization curves for the cases studied.

5. Conclusions

The problem of predicting the thermal degradation of MLI and its effects on the pressure build-up within liquid hydrogen tanks exposed to fires was addressed by developing a transient state model based on thermal node discretization. This takes into account the MLI degradation by assuming that a layer is destroyed when it reaches its melting point. The results obtained from the application of such approach to a realistic case study demonstrate the strong effect of the insulation system degradation on the tank pressurization in fire scenarios. In this situation, the response is similar to the one of an unprotected tank rather than one with an intact insulation system. The results presented in this work require further confirmation from laboratory and large scale tests which, unfortunately, are still not available. Furthermore, it is worth remarking that the proposed approach assumes a quite simple MLI degradation mechanism, which requires further investigation. Nevertheless, the analysis of the case studies shows that the development of models aiming at simulating the behavior of liquid hydrogen tanks to fire exposure cannot neglect the phenomenon of insulation system degradation. The same is true for manufacturers and regulators willing to ensure the safe design and operation of liquid hydrogen tanks.

Nomenclature

T = temperature, K
T_{BB_fire} = fire black body temperature, K
P = pressure, Pa
P_c = critical pressure, Pa
N = number of radiative layers, -
c_p = specific heat capacity at constant pressure, J/(kg·K)
h = convective heat transfer coefficient, W/(m^2·K)
R = universal gas constant, J/(mol·K)
ρ = density, kg/m^3
δ = thickness, m
k = thermal conductivity, W/(m·K)
q = heat flux, W/m^2
M = molecular weight, kg/mol
γ = specific heat ratio, -
σ = Stefan-Boltzmann coefficient, W/(m^2·K^4)
θ = accommodation factor, -
C_2 = empirical constant for the spacer material, -
f = relative density of the spacer to the solid material, -
k_s = thermal conductivity of the spacer material, W/(m·K)
P_r = residual gas pressure within the spacer, Pa
ε = emissivity of the material surface, -
D_x = actual thickness of the spacer, m
m = mass, kg
A_L = internal tank area wetted by the liquid, m^2

References

Anderson C.E., Townsend W., Zook J., Cowgill G., 1974, The effects of fire engulfment on a rail tank car filled with LPG. US Dept Trans.Rept No FRA-OR&D 31–75.

Birk A. M. Otremba F., Gonzalez F., Prabhakaran A., Borch J., Bradley I., Bisby L., 2016, Fire testing of total containment pressure vessels. Chemical Engineering Transactions, 48, 277–282.

Eberwein R., Hajhariri A., Camplese D., Scarponi G.E., Cozzani V., Otremba R.,2023, Insulation materials used in tanks for the storage of cryogenic fluids in fire scenarios. Proceedings of the ASME 2023 Pressure Vessel and Piping Conference (PVP2023).

Edward L., Filip L., 2018, Influence of vacuum level on insulation thermal performance for LNG cryogenic road tankers. MATEC Web of Conferences, 240.

Kunze K., Kircher O., 2012, Cryo-Compressed Hydrogen Storage Cryogenic Cluster Day, Oxford, September 28, 2012. Cryogenic Cluster Day, Oxford (UK), September 28, 2012.

McIntosh, G. E.,1994, Layer by layer MLI calculation using a separated mode equation. Advances in Cryogenic Engineering, 1683–1690.

NIST, 2023, NIST Chemistry WebBook 69, National Institute of Standards and Technology <webbook.nist.gov/chemistry/> accessed on 29.03.2023.

Pehr K., 1996, Experimental examinations on the worst-case behaviour of LH2/LNG tanks for passenger cars. Proceedings of the 11th World Hydrogen Energy Conference, 2169–2187.

Preuster P., Alekseev A., Wasserscheid P., 2017, Hydrogen storage technologies for future energy systems. Annual Review of Chemical and Biomolecular Engineering, 8, 445–471.

Ray M. S., 1994, Coulson and Richardson's Chemical Engineering Volume 6 (Design), 2nd Edition, by R.K. Sinnott, Pergamon Press, Oxford, UK (1993). 954 pages. ISBN 0-08-041865-1. Developments in Chemical Engineering and Mineral Processing, 2(4), 254–255.

Scarponi G. E., Bradley I., Landucci G., Birk A. M., Cozzani V., 2022, Modelling Pressure Tanks under Fire Exposure: Past Experience, Current Challenges and Future Perspectives. Chemical Engineering Transactions, 90, 481–486.

van Wingerden K., Kluge M., Habib A. K., Ustolin F., Paltrinieri N., 2022, Medium-scale Tests to Investigate the Possibility and Effects of BLEVEs of Storage Vessels Containing Liquified Hydrogen. Chemical Engineering Transactions, 90, 547–552.